

# GUIDEd Agents: Enhancing Navigation Policies through Task-Specific Uncertainty Abstraction in Localization-Limited Environments

Gokul Puthumanaim

University of Illinois Urbana-Champaign  
Urbana, Illinois, USA

Email: gokulp2@illinois.edu

Paulo Padrao

Jose Fuentes

Leonardo Bobadilla

Florida International University  
Miami, Florida, USA

Email: {plope113, jfuent099,  
bobadilla}@fiu.edu

Melkior Ornik

University of Illinois Urbana-Champaign  
Urbana, Illinois, USA

Email: mornik@illinois.edu

**Abstract**—Autonomous vehicles performing navigation tasks in complex environments face significant challenges due to uncertainty in state estimation. In many scenarios, such as stealth operations or resource-constrained settings, accessing high-precision localization comes at a significant cost, forcing the robots to rely primarily on less precise state estimates. Our key observation is that different tasks require varying levels of precision in different regions: a robot navigating a crowded space might need precise localization near obstacles but can operate effectively with less precise state estimates in open areas. In this paper, we present a planning method for integrating task-specific uncertainty requirements directly into navigation policies. We introduce Task-Specific Uncertainty Maps (TSUMs), which abstract the acceptable levels of state estimation uncertainty across different regions. TSUMs align task requirements and environmental features using a shared representation space, generated via a domain-adapted encoder. Using TSUMs, we propose Generalized Uncertainty Integration for Decision-Making and Execution (GUIDE), a policy conditioning framework that incorporates these uncertainty requirements into the robot’s decision-making process. We find that TSUMs provide an effective way to abstract task-specific uncertainty requirements, and conditioning policies on TSUMs enables the robot to reason about the context-dependent value of certainty and adapt its behavior accordingly. We show how integrating GUIDE into reinforcement learning frameworks allows the agent to learn navigation policies that effectively balance task completion and uncertainty management without the need for explicit reward engineering. We evaluate GUIDE on a variety of real-world robotic navigation tasks and find that it demonstrates significant improvement in task completion rates compared to baseline methods that do not explicitly consider task-specific uncertainty. Evaluation videos and code are available at <https://guided-agents.github.io>.

## I. INTRODUCTION

In complex environments where robots must balance task completion with resource usage, managing uncertainty in state estimation becomes a critical challenge. Consider an autonomous surface vehicle (ASV) conducting a mapping mission in stealth-critical settings where each GPS fix risks

<sup>1</sup>Marine navigation dataset will be made available on the website after the anonymous review period.

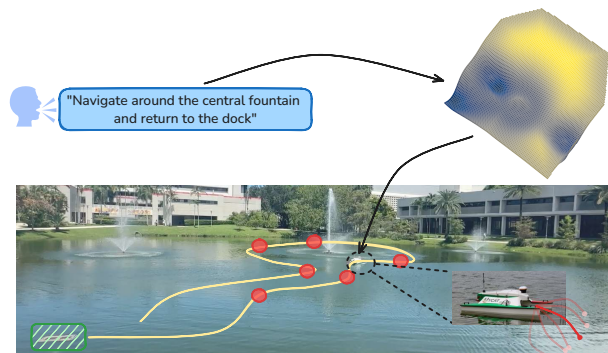


Fig. 1: Illustration of our method applied to a robotic navigation task in a localization-limited environment. Top Left: The ASV is assigned a navigation task. Top Right: GUIDE interprets the task and generates a representation highlighting areas where the ASV needs higher positional certainty (dark blue). Bottom: The policy executed by the ASV. The white line represents the trajectory taken by the ASV towards the dock (green rectangle), the red dots indicate locations where the ASV actively reduces its state estimation uncertainty to satisfy task-specific requirements.

detection, or a ground robot operating in environments where high-precision localization requires costly computation. In such resource-constrained settings, the robot must not only complete its assigned task but also carefully manage when and where to use expensive localization operations. Importantly, constantly striving to reduce uncertainty through high-precision localization is neither necessary nor efficient for successful task execution. When operating in regions critical to the task objectives or near obstacles, precise localization becomes crucial for mission success. However, in areas less relevant to the immediate task goals, the robot can often tolerate higher positional uncertainty, allowing it to focus on efficient task execution rather than achieving pinpoint

accuracy. This scenario underscores a fundamental challenge in robotic navigation: in environments with limited access to high-precision localization, the robot must balance task completion with uncertainty management, where the acceptable level of uncertainty at any location is inherently *task-specific* and *context-dependent*.

Traditional approaches to navigation in environments with limited access to high-precision localization often fall into two categories: minimizing uncertainty universally through frequent use of expensive localization [47, 12, 37, 13] or enforcing fixed uncertainty thresholds across the environment [7, 19, 52]. While these strategies may be effective in settings where localization resources are abundant, they become impractical when high-precision state estimation comes at a cost. For instance, in stealth-critical missions, universally enforcing precise localization through frequent GPS usage would compromise the robot’s coyness, even in regions where such precision isn’t necessary for task execution.

Existing methods also struggle to balance resource usage with task requirements. While some approaches attempt to reduce localization costs by considering task performance [65, 63], they typically apply a uniform trade-off across all situations. This fails to account for how the value of precise localization varies across different phases of the mission. Furthermore, these methods often require extensive reward engineering to capture the complex relationship between task objectives and localization costs [77, 5].

The fundamental issue lies in the disconnect between task requirements and resource-constrained uncertainty management. Current frameworks treat localization decisions independently from task specifications, leading to either excessive resource consumption or compromised task performance when different regions demand different levels of certainty.

**Statement of contributions:** With the aim of bridging the gap between high-level task descriptions and low-level uncertainty handling, we propose the concept of a *Task-Specific Uncertainty Map (TSUM)*. A TSUM serves as an intermediate abstraction that represents the acceptable levels of state estimation uncertainty across different regions of the environment for a specific task. We present a CLIP-based approach for computing TSUMs that effectively aligns visual environmental features with textual task specifications in a shared embedding space.

Building upon TSUM, we introduce *Generalized Uncertainty Integration for Decision-Making and Execution (GUIDE)*, a policy conditioning framework that incorporates TSUMs into navigation policies. The core proposition of GUIDE is that by conditioning navigation policies on these task-specific uncertainty requirements, robots can better reason about the *context-dependent value of certainty*. This enables the generation of policies that dynamically adapt their behavior based on the varying uncertainty requirements across different regions of the environment.

Finally, we demonstrate how GUIDE can be integrated into a reinforcement learning framework. Specifically, we adapt the Soft Actor-Critic algorithm, resulting in the *GUIDEd Soft*

*Actor-Critic (G-SAC)* method. G-SAC learns navigation policies that effectively balance task completion and uncertainty management without the need for explicit reward engineering tailored to each specific task.

We evaluate GUIDE in the context of marine autonomy using Autonomous Surface Vehicles (ASVs). We chose marine navigation as our experimental domain for three key reasons: (i) marine navigation presents inherently greater challenges than ground navigation due to environmental uncertainty from waves, currents, and weather conditions, (ii) it enables evaluation through real-world, ‘in-the-wild’ deployment rather than controlled laboratory settings, and (iii) it represents a less-explored area in robotics with limited datasets and established benchmarks. Our experimental results show significant improvements in task performance when compared to state-of-the-art methods that do not explicitly consider task-specific uncertainty requirements.

## II. RELATED WORKS

*a) Uncertainty Modeling in Robotic Navigation:* Uncertainty management is a fundamental aspect of robotic navigation, where robots must make decisions based on imperfect information about their state and the environment [47, 57]. Probabilistic techniques such as Bayesian filters [15, 25, 39] and particle filters [16, 66, 11] have been widely used to enable robust localization and mapping in stochastic environments. These methods allow robots to estimate their position and navigate effectively despite sensor noise and environmental uncertainties. However, traditional approaches often treat uncertainty uniformly across the environment, without considering how different regions may require varying levels of certainty depending on the navigation task. While these methods effectively estimate and track uncertainty, they are not designed for scenarios where reducing uncertainty comes at a significant cost. In resource-constrained environments where high-precision localization is limited, simply estimating uncertainty is insufficient - robots must also reason about when to invest in reducing it.

*b) Reinforcement Learning for Navigation:* Reinforcement Learning (RL) has been successfully applied to robotic navigation tasks, enabling agents to learn navigation policies through interaction with the environment [69, 70, 75]. Standard RL algorithms have been used to train robots to navigate in various settings, from simulated environments to real-world scenarios [31, 74, 67]. While these methods can learn effective policies in controlled environments [79, 46, 27], they often perform suboptimally in real-world scenarios due to factors like partial observability, dynamic changes, and varying levels of uncertainty [8, 38]. Additionally, standard RL typically does not account for uncertainty explicitly, which can hinder performance in complex environments where uncertainty plays a significant role. Moreover, lot of these methods typically assume unbounded access to state information, making them poorly suited for environments where precise state estimation is a limited resource that must be strategically utilized.

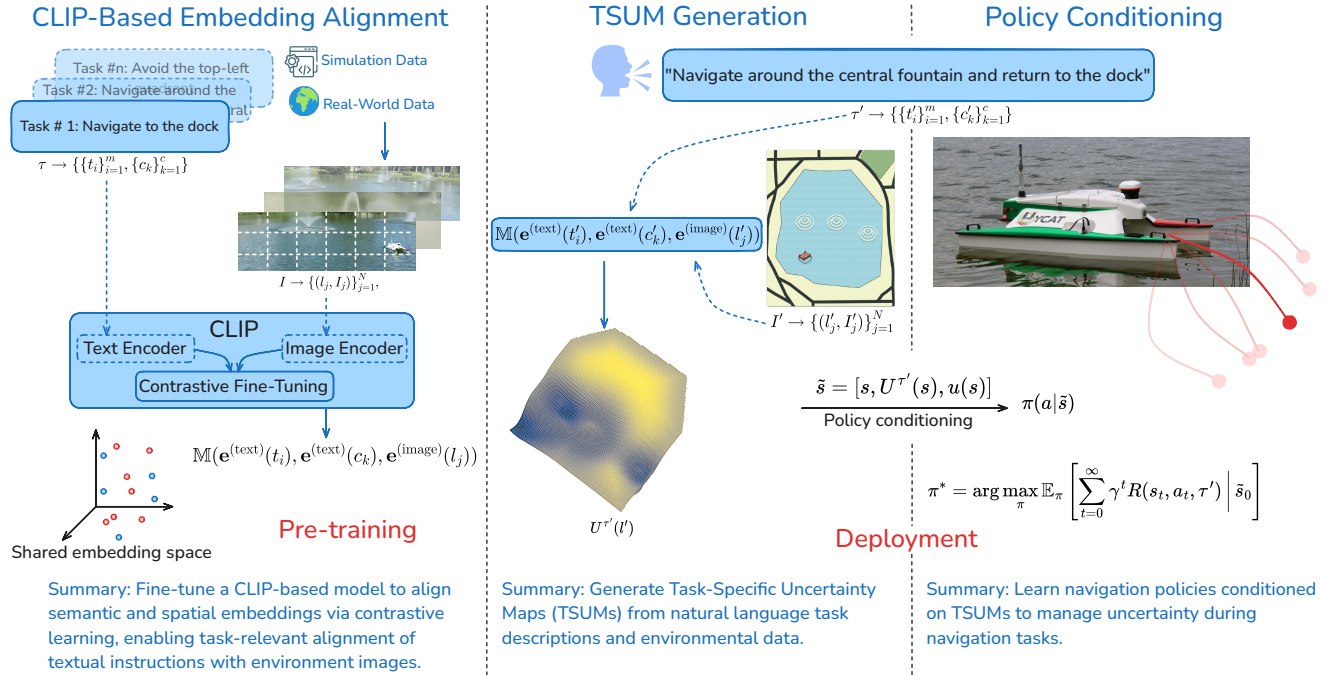


Fig. 2: Overview of GUIDE. The framework consists of two phases: Embedding Alignment (Pre-training) and Deployment. In the embedding alignment phase, semantic and spatial embeddings are fine-tuned and aligned using a CLIP-based model with contrastive learning. During deployment, TSUMs are generated from natural language task descriptions and environmental data, and navigation policies are conditioned on these TSUMs to manage uncertainty in a task-aware manner.

*c) Task-Specific Navigation Policies:* Recent advances have focused on developing navigation policies that are conditioned on specific tasks or goals [51, 10, 41, 36]. Task-conditioned RL allows agents to adapt their behavior based on high-level task specifications, improving flexibility and generalization. In navigation, this has been explored by training policies capable of handling objectives, adjusting the robot's behavior according to the task [78, 68, 40]. These approaches often neglect the varying importance of uncertainty management [9, 26] across different tasks and environments.

*d) Uncertainty-Aware Reinforcement Learning in Navigation:* Incorporating uncertainty into RL for navigation has been investigated to enhance exploration, robustness, and safety [62, 75]. Some approaches introduce uncertainty penalization directly into the reward function, encouraging agents to avoid high-uncertainty regions [14, 76, 33]. Others utilize Bayesian RL methods to model uncertainty in value estimation, improving decision-making under uncertainty [3, 1]. Bootstrapped ensembles maintain multiple value function estimates to capture epistemic uncertainty, leading to more informed exploration strategies [43, 2, 28, 71]. While these methods consider uncertainty, they often do so globally or uniformly [48, 30, 44] across the environment and do not tailor the uncertainty management to specific navigation tasks or spatial regions. This uniform treatment of uncertainty becomes particularly problematic in resource-constrained settings, where robots have limited opportunities

to reduce uncertainty. These methods lack mechanisms to reason about when consuming these limited resources would provide the most value for task completion.

*e) Risk-Aware Planning and Navigation:* Risk-aware planning introduces measures to balance performance and safety by considering the potential risks associated with different actions [32, 18]. These techniques [42, 73] enable robots to make decisions that account for uncertainty in the environment [22]. In the context of RL, risk-sensitive approaches adjust the policy to avoid high-risk actions, often through modified reward functions or policy constraints [6, 35, 64]. Although effective in managing risk, these methods typically apply uniform risk thresholds and do not adapt to the task-specific uncertainty requirements that may vary across different navigation scenarios.

*f) Task-Specific Uncertainty Management in Navigation:* Integrating high-level task specifications into uncertainty management for navigation remains an open challenge. Some recent works propose large pre-trained models to interpret complex instructions and generate corresponding navigation behaviors [59, 45, 61, 21, 60, 58, 4]. While these approaches enable robots to understand and execute a wider range of tasks, they often lack a systematic method for representing and integrating task-specific uncertainty requirements into the navigation policy. This limitation reduces their effectiveness in complex environments where the importance of uncertainty can vary significantly across different regions.

In contrast to prior works, we place our research at the intersection of task-specific navigation and resource-constrained uncertainty management. Our proposed GUIDE framework addresses a critical gap in existing literature: how to effectively navigate in environments where high-precision localization is a limited resource that must be strategically utilized. While previous approaches either assume unlimited access to precise state estimation or treat uncertainty uniformly across tasks, GUIDE systematically incorporates both task requirements and localization constraints into the navigation policy. By providing a principled way to reason about when and where to use costly localization operations, our approach enables robots to dynamically balance task completion with resource usage, adapting their behavior based on the varying importance of uncertainty across different regions of the environment.

### III. THE GUIDE FRAMEWORK

Consider a robot operating in a continuous state space  $\mathcal{S}$ , where each state  $s \in \mathcal{S}$  encodes the robot’s pose. The robot can execute control inputs from a continuous action space  $\mathcal{A}$ . Operating in a localization-limited environment, the robot’s state estimate is subject to uncertainty due to sensor noise, communication constraints, and environmental factors. While the robot can access high-precision localization readings, doing so incurs significant costs—for instance, an autonomous surface vehicle (ASV) conducting stealth-critical missions where each GPS fix risks detection, or a ground robot in environments where precise localization demands substantial computational resources.

We assume the availability of a visual representation of the operating environment *a priori*, such as an overhead map or imagery covering the region of interest. This assumption is justified in many real-world applications where survey data or geographic information systems provide baseline knowledge of the environment (e.g., topography, known obstacles).

A *navigation task*  $\tau$ , specified in natural language, describes the robot’s objectives and associated constraints with respect to environmental features. For example,  $\tau$  might require the robot to “navigate to the dock while avoiding right quadrant”. The essential characteristic is that these tasks reference spatial or semantic features describing the environment.

*Objective:* Synthesize a navigation policy  $\pi(a | s)$  that enables task completion while explicitly reasoning about the robot’s state-estimation uncertainty  $u(s)$ . The policy must balance two competing demands: efficient task execution and strategic uncertainty management. This balance is particularly crucial in resource-constrained settings where reducing uncertainty comes at a significant cost.

To achieve this objective, the GUIDE framework addresses two fundamental challenges in uncertainty-aware navigation:

- (i) *Task Interpretation:* Given a natural language task  $\tau$ , determine acceptable levels of uncertainty across different regions of the environment. This interpretation captures how important precise state estimation is for each area of the operating space, based on task requirements and environmental features.

- (ii) *Policy Synthesis:* Generate a navigation policy that incorporates task-specific uncertainty requirements into its decision-making process. This policy should prioritize uncertainty reduction in critical regions while efficiently pursuing task objectives where precise localization is less crucial.

Fig. 2 presents an overview of the GUIDE framework. In the following sections, we detail how these components are implemented within a unified navigation architecture.

#### A. Task-Specific Uncertainty Map (TSUM)

To effectively integrate task-specific uncertainty considerations into robotic navigation policies, we introduce the abstraction of *Task-Specific Uncertainty Maps* (TSUMs). A TSUM serves as an intermediate representation that bridges the gap between high-level task specifications and low-level uncertainty management decisions. Formally, a TSUM is a function  $U^\tau : L \rightarrow \mathbb{R}^+$  that assigns an acceptable level of state estimation uncertainty to each location  $l \in L$  for a given navigation task  $\tau$ .

The TSUM  $U^\tau(l)$  is defined as:

$$U^\tau(l) = w_\Phi \Phi^\tau(l) + w_C C^\tau(l) + w_E \mathcal{E}(l), \quad (1)$$

where  $\Phi^\tau(l)$  quantifies the task-specific importance of location  $l$ ,  $C^\tau(l)$  represents task constraints at  $l$ , and  $\mathcal{E}(l)$  captures environmental factors. The weights  $w_\Phi$ ,  $w_C$ , and  $w_E$  control the relative influence of each component, allowing us to balance different aspects of the task and environment. These weights are determined through validation on a held-out dataset of annotated scenarios<sup>2</sup>. By encoding the varying importance of uncertainty reduction across different regions of the environment, we provide a task-oriented abstraction of acceptable levels of state-estimation uncertainty that can be used to guide navigation policies.

1) *CLIP-Based TSUM Generation Pipeline:* To generate TSUMs that effectively capture the relationship between visual environment features and task requirements, we propose a vision-language approach using the CLIP (Contrastive Language-Image Pre-training) model [50]. Our pipeline processes both visual and textual inputs to produce a spatially-varying uncertainty map. The following sections detail how we process environmental information and task specifications to compute each component of the TSUM, leveraging CLIP’s powerful cross-modal understanding capabilities.

a) *Environment Representation:* As established in Section III, we assume access to a visual representation of the operating environment through overhead imagery. To process this spatial information systematically, we discretize the continuous space  $L$  into a grid of  $N$  image patches  $\{I_1, I_2, \dots, I_N\}$ , where each patch  $I_j$  corresponds to a discrete spatial region  $l_j \subset L$ . The discretization parameters are chosen to balance computational efficiency with feature preservation.

<sup>2</sup>The dataset was collected using an Autonomous Surface Vehicle in a controlled environment. Details are provided in the supplementary. The dataset will be open-sourced after the review period.

b) *Task Processing*: Given a navigation task  $\tau$  specified in natural language, we employ a hierarchical parsing approach to extract structured task representations. We utilize a dependency parser with a context-free grammar [55, 23] to decompose  $\tau$  into atomic statements that capture both objectives and their associated constraints. These atomic statements are then organized into  $m$  primary specifications  $\{t_i\}_{i=1}^m$  and  $c$  auxiliary specifications  $\{c_k\}_{k=1}^c$ , allowing for natural coupling between objectives and their execution requirements.

c) *CLIP Encoding*: We leverage CLIP’s vision-language architecture to project both spatial and semantic information into a shared representational space. The model consists of two parallel encoders:

$$E_{\text{text}} : \mathcal{T} \rightarrow \mathbb{R}^d, \quad E_{\text{image}} : \mathcal{I} \rightarrow \mathbb{R}^d \quad (2)$$

where  $\mathcal{T}$  and  $\mathcal{I}$  denote the spaces of tokenized text and normalized image patches respectively, and  $d = 512$  matches CLIP’s native embedding dimension chosen to optimize the balance between representational capacity and computational efficiency. These encoders employ self-attention mechanisms and cross-modal transformers to generate context-aware embeddings  $\mathbf{e}^{(\text{text})}(t_i), \mathbf{e}^{(\text{text})}(c_k) \in \mathbb{R}^d$  for textual components and  $\mathbf{e}^{(\text{image})}(l_j) \in \mathbb{R}^d$  for spatial regions.

d) *Cross-Modal Alignment*: The shared embedding space facilitates direct semantic comparison between task specifications and environmental features through cosine similarity [54]:

$$\text{sim}(t, l) = \text{cosine}(\mathbf{e}^{(\text{text})}(t), \mathbf{e}^{(\text{image})}(l))$$

This metric quantifies the semantic relevance between spatial regions and task components, enabling the construction of spatially-varying relevance maps. While CLIP’s pre-training on diverse image-text pairs provides robust general-purpose understanding, domain-specific applications may benefit from additional fine-tuning. In our implementation, we fine-tune the last six transformer layers on a navigation dataset when deploying in maritime environments (details in Section III-A3b).

The complete pipeline (illustrated in Fig. 3) processes environmental and task information in parallel streams, combining them through the CLIP embeddings. The following section details how these embeddings are used to compute task relevance and constraint components, which are then aggregated to generate the final TSUM representing acceptable uncertainty thresholds across the environment.

2) *Computing Task Relevance and Constraints*: Having established our CLIP-based pipeline, we now detail how we compute each component of the TSUM. Our approach leverages the rich semantic understanding captured by CLIP’s shared embedding space to quantify task relevance and constraints at each location.

Using the encoder functions defined in Equation (2), we obtain embeddings ( $\mathbf{e}^{(\text{text})}(t_i), \mathbf{e}^{(\text{text})}(c_k) \in \mathbb{R}^d$  for text and  $\mathbf{e}^{(\text{image})}(l_j) \in \mathbb{R}^d$  for image patches) that capture the semantic features of both textual descriptions and visual characteristics in a shared  $d$ -dimensional space. This shared representation allows us to meaningfully compare how well visual features

at each location align with the requirements expressed in the task description.

a) *Task Relevance Function  $\Phi^\tau(l)$* : To compute the task relevance at each location, we first calculate similarity scores between each subtask and location

$$\rho_{t_i}(l_j) = \text{cosine}(\mathbf{e}^{(\text{text})}(t_i), \mathbf{e}^{(\text{image})}(l_j)). \quad (3)$$

These raw similarities are converted to attention weights using a softmax operation

$$\alpha_i(l_j) = \frac{\exp(\rho_{t_i}(l_j))}{\sum_{i'=1}^m \exp(\rho_{t_{i'}}(l_j))}.$$

The task relevance function  $\Phi^\tau(l_j)$  is then computed as a weighted sum

$$\Phi^\tau(l_j) = \sum_{i=1}^m \alpha_i(l_j) \rho_{t_i}(l_j).$$

This formulation creates a natural prioritization mechanism – locations that strongly match with important subtasks receive higher relevance scores. The attention weights  $\alpha_i$  ensure that the most pertinent subtasks for each location dominate the relevance calculation, while the weighted sum combines evidence from all subtasks proportional to their importance.

b) *Constraint Function  $\mathcal{C}^\tau(l)$* : We follow a similar procedure for computing constraint relevance. For each constraint  $c_k$ , we compute

$$\rho_{c_k}(l_j) = \text{cosine}(\mathbf{e}^{(\text{text})}(c_k), \mathbf{e}^{(\text{image})}(l_j)).$$

Constraint attention weights are computed as

$$\beta_k(l_j) = \frac{\exp(\rho_{c_k}(l_j))}{\sum_{k'=1}^c \exp(\rho_{c_{k'}}(l_j))}.$$

The final constraint function aggregates these weighted similarities

$$\mathcal{C}^\tau(l_j) = \sum_{k=1}^c \beta_k(l_j) \rho_{c_k}(l_j).$$

Higher values of  $\mathcal{C}^\tau(l_j)$  indicate locations where constraints are particularly relevant and uncertainty management is critical.

c) *Environmental Factors  $\mathcal{E}(l)$* : While CLIP embeddings capture visual features, certain navigation-relevant attributes may not be directly observable from imagery. We incorporate these additional factors through a vector of environmental features  $\text{env\_features}(l_j) \in \mathbb{R}^p$ , which encodes relevant spatial properties from auxiliary data sources. These features are mapped to a scalar value through

$$\mathcal{E}(l_j) = w_{\text{env}}^\top \text{env\_features}(l_j) + b_{\text{env}},$$

where  $w_{\text{env}} \in \mathbb{R}^p$  and  $b_{\text{env}} \in \mathbb{R}$  are learned parameters optimized during training.

The final TSUM value at each location is computed by combining these components according to Equation (1).

3) *Implementation Details*: We now present the practical details of our implementation, including dataset preparation, model fine-tuning, and training procedures.

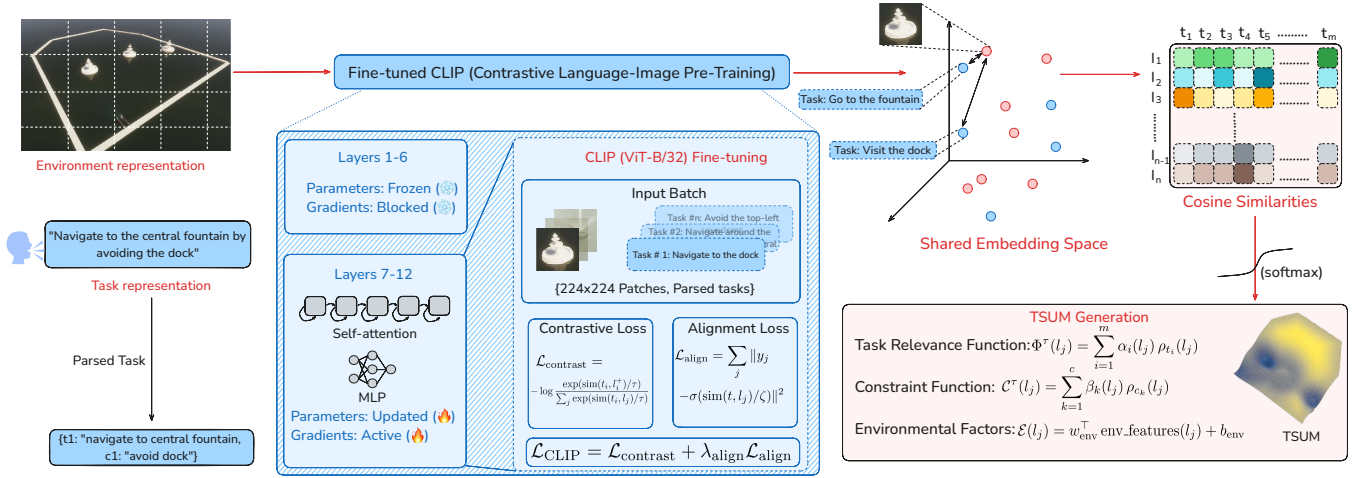


Fig. 3: CLIP-based TSUM generation pipeline. The environment image and task description are processed through a fine-tuned CLIP model to obtain embeddings in a shared semantic space. These embeddings are used to compute attention-weighted task relevance and constraint components, which are combined with environmental factors to generate the final TSUM representing acceptable uncertainty levels across the environment.

a) *Dataset*: Our training dataset consists of 2,500 annotated overhead images collected from both real-world environments and high-fidelity simulations, covering a diverse range of navigation scenarios in a freshwater lake environment. Each image patch is discretized to  $224 \times 224$  pixels at 0.5 meters per pixel resolution, chosen to align with CLIP’s architecture while preserving sufficient detail for navigation-relevant feature extraction. Each patch is annotated with:

$$\mathcal{D} = \{(I_j, l_j, y_j^t, y_j^c, f_j)\}_{j=1}^N,$$

where  $I_j$  is the image patch,  $l_j$  represents location coordinates,  $y_j^t$  and  $y_j^c$  are binary relevance labels for a predefined set of subtasks and constraints respectively, and  $f_j$  contains environmental features including bathymetry, static obstacles, and known traffic patterns. The dataset is split into 2,000 images for training and 500 for validation.

b) *CLIP Fine-tuning*: We adopt a selective fine-tuning approach to adapt the pre-trained CLIP (ViT-B/32) model while preserving its general vision-language understanding. Specifically, we freeze the first six transformer layers to maintain CLIP’s foundational cross-modal understanding, while fine-tuning the remaining six layers to adapt to navigation-specific concepts. We optimize the following loss function:

$$\mathcal{L}_{\text{CLIP}} = \mathcal{L}_{\text{contrast}} + \lambda_{\text{align}} \mathcal{L}_{\text{align}},$$

where  $\mathcal{L}_{\text{contrast}}$  is the standard CLIP contrastive loss

$$\mathcal{L}_{\text{contrast}} = -\log \frac{\exp(\text{sim}(t_i, l_i^+)/\tau)}{\sum_j \exp(\text{sim}(t_i, l_j)/\tau)},$$

and  $\mathcal{L}_{\text{align}}$  is an additional alignment loss that encourages consistency between expert labels and embedding similarities

$$\mathcal{L}_{\text{align}} = \sum_j \|y_j - \sigma(\text{sim}(t, l_j)/\zeta)\|^2.$$

Here,  $\zeta$  is a temperature parameter set to 0.07, and  $\sigma$  is the sigmoid function. We freeze the first six transformer layers of CLIP and fine-tune the remaining layers for 10 epochs using AdamW optimizer with a learning rate of  $1e-5$ .

c) *Training Procedure*: The complete training process involves three stages:

- (i) We fine-tune CLIP using  $\mathcal{L}_{\text{CLIP}}$  as described above.
- (ii) We train the environmental feature weights  $w_{\text{env}}$  and  $b_{\text{env}}$  by minimizing

$$\mathcal{L}_{\text{env}} = \sum_j \|\mathcal{E}(l_j) - \hat{e}_j\|^2,$$

where  $\hat{e}_j$  represents ground truth annotations derived from auxiliary spatial data.

- (iii) Finally, we optimize the component weights  $w_{\Phi}$ ,  $w_C$ , and  $w_{\mathcal{E}}$  using a validation set of TSUMs

$$\mathcal{L}_{\text{TSUM}} = \sum_j \|U^\tau(l_j) - U_{\text{ref}}^\tau(l_j)\|^2.$$

The reference TSUMs ( $U_{\text{ref}}^\tau$ ) were generated using a combination of automated and manual annotation processes. We utilized a high-fidelity Unity-based simulation environment to automatically generate initial uncertainty requirements based on task execution traces. These were then refined through a systematic review process to ensure alignment with navigation requirements. During training, we employ early stopping based on validation performance with a patience of 5 epochs. Data augmentation includes random rotations and flips of the image patches to improve robustness. The pipeline is implemented in PyTorch, with compute-intensive operations accelerated using TorchScript for optimal GPU utilization. Training is performed on NVIDIA A100 GPUs in a distributed setting using PyTorch’s DistributedDataParallel, with environment

simulation and data generation parallelized across multiple nodes to maximize throughput.

### B. Conditioning Navigation Policies Using Task-Specific Uncertainty Maps

To enable robots to manage uncertainty in a task-aware manner, we propose conditioning the navigation policy on the Task-Specific Uncertainty Map (TSUM). Our objective is to learn a policy  $\pi$  that allows the robot to efficiently accomplish the task  $\tau$  while adhering to the uncertainty requirements specified by the TSUM.

To condition the policy, we augment the state representation to include both the acceptable uncertainty levels from the TSUM and the robot’s current estimation of its state uncertainty. For a given task  $\tau$ , the augmented state  $\tilde{s}$  is defined as:

$$\tilde{s} = [s, U^\tau(s), u(s)],$$

where  $s$  is the original state representing the robot’s observation of the environment,  $U^\tau(s)$  is the acceptable uncertainty level at state  $s$  derived from the TSUM, and  $u(s)$  is the robot’s current state estimation uncertainty.

By conditioning the policy  $\pi(a|\tilde{s})$  on the augmented state  $\tilde{s}$ , the agent makes decisions based not only on the environmental state but also on the acceptable, actual and future uncertainty levels at each location. This allows the agent to adjust its actions to meet the task-specific uncertainty requirements.

The reinforcement learning problem is formulated in the augmented state space. The objective is to learn an optimal policy  $\pi^*(a|\tilde{s})$  that maximizes the expected cumulative reward:

$$\pi^* = \arg \max_{\pi} \mathbb{E}_{\pi} \left[ \sum_{t=0}^{\infty} \gamma^t R(s_t, a_t, \tau) \mid \tilde{s}_0 \right],$$

where  $\gamma \in [0, 1)$  is the discount factor, and  $R(s_t, a_t, \tau)$  is the task-specific reward function.

Standard reinforcement learning algorithms can be employed to solve this optimization problem in the augmented state space. In the next section, we show how a standard RL algorithm can be adapted using our framework.

1) *GUIDEd Soft Actor-Critic Algorithm*: While any reinforcement learning algorithm can be used to learn the optimal policy  $\pi^*(a|\tilde{s})$ , we adopt the Soft Actor-Critic (SAC) algorithm [17] due to its sample efficiency and robustness. Our adapted version, referred to as *GUIDEd SAC*, integrates TSUMs by conditioning the policy and value functions on the augmented state  $\tilde{s}$ .

In the SAC framework, the objective is to maximize the expected cumulative reward augmented by an entropy term, which encourages exploration:

$$J(\pi) = \mathbb{E}_{\pi} \left[ \sum_{t=0}^{\infty} \gamma^t (R(s_t, a_t, \tau) + \alpha \mathcal{H}(\pi(\cdot|\tilde{s}_t))) \mid \tilde{s}_0 \right],$$

where  $\mathcal{H}(\pi(\cdot|\tilde{s}_t)) = -\mathbb{E}_{a_t \sim \pi(\cdot|\tilde{s}_t)} [\log \pi(a_t|\tilde{s}_t)]$  is the entropy of the policy at state  $\tilde{s}_t$ , and  $\alpha$  is the temperature parameter balancing exploration and exploitation.

GUIDEd SAC maintains parameterized function approximators for the policy  $\pi_{\theta}(a|\tilde{s})$  and the soft Q-value functions  $Q_{\phi_1}(\tilde{s}, a)$  and  $Q_{\phi_2}(\tilde{s}, a)$ , where  $\theta$  and  $\phi_i$  denote the parameters of the policy and value networks, respectively.

The soft Q-value networks  $Q_{\phi_i}(\tilde{s}, a)$  are updated by minimizing the soft Bellman residual:

$$\mathcal{L}_Q(\phi_i) = \mathbb{E}_{(\tilde{s}_t, a_t, r_t, \tilde{s}_{t+1}) \sim \mathcal{D}} \left[ (Q_{\phi_i}(\tilde{s}_t, a_t) - y_t)^2 \right], \quad (4)$$

where  $\mathcal{D}$  is the replay buffer, and the target value  $y_t$  is computed as:

$$y_t = r_t + \gamma \left( \min_{i=1,2} Q_{\bar{\phi}_i}(\tilde{s}_{t+1}, a_{t+1}) - \alpha \log \pi_{\theta}(a_{t+1}|\tilde{s}_{t+1}) \right), \quad (5)$$

with  $a_{t+1} \sim \pi_{\theta}(\cdot|\tilde{s}_{t+1})$  and  $Q_{\bar{\phi}_i}$  being the target Q-value networks with delayed parameters for stability.

The policy network  $\pi_{\theta}(a|\tilde{s})$  is updated by minimizing:

$$\mathcal{L}_{\pi}(\theta) = \mathbb{E}_{\tilde{s}_t \sim \mathcal{D}} \left[ \mathbb{E}_{a_t \sim \pi_{\theta}(\cdot|\tilde{s}_t)} [\alpha \log \pi_{\theta}(a_t|\tilde{s}_t) - Q_{\phi}(\tilde{s}_t, a_t)] \right], \quad (6)$$

where  $Q_{\phi}(\tilde{s}_t, a_t) = \min_{i=1,2} Q_{\phi_i}(\tilde{s}_t, a_t)$ .

The temperature parameter  $\alpha$  is adjusted by minimizing:

$$\mathcal{L}(\alpha) = \mathbb{E}_{a_t \sim \pi_{\theta}(\cdot|\tilde{s}_t)} \left[ -\alpha (\log \pi_{\theta}(a_t|\tilde{s}_t) + \bar{\mathcal{H}}) \right], \quad (7)$$

where  $\bar{\mathcal{H}}$  is the target entropy. Algorithm 1 summarizes the GUIDEd SAC algorithm.

---

#### Algorithm 1 GUIDEd SAC Algorithm

---

- 1: **Initialize** policy network  $\pi_{\theta}(a|\tilde{s})$ , Q-value networks  $Q_{\phi_1}$ ,  $Q_{\phi_2}$ , target Q-value networks  $Q_{\bar{\phi}_1}$ ,  $Q_{\bar{\phi}_2}$ , temperature parameter  $\alpha$ , and replay buffer  $\mathcal{D}$ .
  - 2: **for** each environment interaction step **do**
  - 3:   Obtain current state  $s_t$ , acceptable uncertainty  $U^\tau(s_t)$ , current uncertainty  $u(s_t)$ .
  - 4:   Form augmented state  $\tilde{s}_t = [s_t, U^\tau(s_t), u(s_t)]$ .
  - 5:   Sample action  $a_t \sim \pi_{\theta}(\cdot|\tilde{s}_t)$ .
  - 6:   Execute action  $a_t$ , observe reward  $r_t$  and next state  $s_{t+1}$ .
  - 7:   Compute  $\tilde{s}_{t+1} = [s_{t+1}, U^\tau(s_{t+1}), u(s_{t+1})]$ .
  - 8:   Store transition  $(\tilde{s}_t, a_t, r_t, \tilde{s}_{t+1})$  in replay buffer  $\mathcal{D}$ .
  - 9: **end for**
  - 10: **for** each gradient step **do**
  - 11:   Sample minibatch of transitions from  $\mathcal{D}$ .
  - 12:   Update Q-value networks  $Q_{\phi_i}$  by minimizing  $\mathcal{L}_Q(\phi_i)$  (Equation (4)).
  - 13:   Update policy network  $\pi_{\theta}$  by minimizing  $\mathcal{L}_{\pi}(\theta)$  (Equation (6)).
  - 14:   Adjust temperature parameter  $\alpha$  by minimizing  $\mathcal{L}(\alpha)$  (Equation (7)).
  - 15:   Update target Q-value networks:  $\bar{\phi}_i \leftarrow \tau \phi_i + (1-\tau)\bar{\phi}_i$ .
  - 16: **end for**
- 

## IV. EXPERIMENTS

*Motivating scenario*: Consider a stealth reconnaissance mission where an autonomous vehicle must navigate through

previously unexplored waters. The vehicle can either rely on passive, noisy sensors or risk detection by activating high-precision GPS. Each GPS usage increases the chance of compromising the mission, yet completing the assigned tasks requires maintaining sufficient localization accuracy in critical regions.

To evaluate GUIDEd agents in such challenging scenarios, we conduct experiments using an autonomous surface vehicle (ASV) in real-world, previously unseen environments. The ASV is tasked with executing a set of navigation tasks that it has never encountered during training. Operating in a GPS-constrained setting, the ASV must strategically manage its localization resources: by default, it relies on passive sensors providing noisy position estimates, but can request precise GPS fixes at the cost of increased mission risk. The experimental setup is designed to capture realistic operational constraints [49, 72] where robots must balance competing objectives. Relying solely on noisy localization can lead to task failure in regions requiring precision, while excessive use of GPS not only increases mission costs but could compromise stealth objectives.

#### A. Experimental Setup

1) *Environment*: The ASV operates in an open lake characterized by environmental variability and human-induced disturbances. The environment features fountains that serve as obstacles and introduce additional layers of uncertainty by generating water disturbances that create both physical challenges for navigation and contribute to the overall uncertainty in state estimation.

2) *Autonomous Surface Vehicle Setup*: Our experiments utilize the SeaRobotics Surveyor Autonomous Surface Vehicle (ASV), which is equipped with a Global Positioning System (GPS), an Inertial Measurement Unit (IMU), and a YSI EXO2 multiparameter water quality sonde. The GPS provides precise positioning, while the IMU assists with motion tracking and orientation. The YSI EXO2 sonde, primarily used for environmental monitoring, contributes to the overall state estimation by providing additional context.

The action space of the ASV is defined as  $a = (\lambda, \alpha, \eta)$ , where  $\lambda \in [0, \lambda_{\max}]$  represents the propulsion torque (with  $\lambda_{\max}$  being the maximum allowed torque),  $\alpha \in [0, 2\pi)$  denotes the steering angle, and  $\eta$  is a discrete variable indicating the mode of position estimation. The ASV has a maximum speed of 2 knots.

3) *Position Estimation Modes*: To represent the operational challenges of managing uncertainty during navigation, we model two modes of position estimation for the ASV [49]:

- (i) **Noisy Position Estimation**: By default, the ASV estimates its position using the IMU and YSI EXO2 sensors, which results in a noisy and less accurate position estimate [53]. This mode represents the low-cost but high-uncertainty estimate.
- (ii) **Exact Position Estimation**: The ASV can request exact position data from GPS. This incurs a higher resource cost, leading to a reduced overall mission reward.

The reward structure is designed to encourage task completion while balancing the efficient management of positional uncertainty, without biasing the results in favor of GUIDE compared to the baselines. The reward function for task execution,  $r_{\text{task}}$ , incentivizes mission completion, while each use of exact position estimation incurs a penalty  $c_{\text{exact}}$  to reflect its associated cost. Conversely, noisy estimation incurs a smaller penalty  $c_{\text{noisy}}$ , encouraging the ASV to balance accuracy needs with operational efficiency.

4) *Evaluation Protocol*: The agent receives a natural language task specification, describing a navigation task using key features of the environment. Task completion is evaluated based on specific criteria for each task type. For goal-reaching tasks, the agent must reach within a 1.5-meter radius of the target. For perimeter or exploration tasks, it must remain within a 3.5-meter corridor of the path, and for avoid tasks, a 3-meter minimum distance from designated areas is required. Task completion rate (TCR) is determined by the proportion of the task completed, and rewards are based on the total reward earned at task completion. All baselines interpret instructions through the same semantic parser, converting them into structured representations suitable for each algorithm.

#### B. Baselines and Ablations

We compare GUIDE against several baselines and conduct ablation studies.

1) *Ablation Studies*: We perform two ablations:

- (i) *Standard RL without TSUMs (SAC, Ablation 1)*: We train SAC agents using only the original state  $s$ , without TSUMs, to assess the importance of TSUMs in managing uncertainty.
- (ii) *GUIDEd PPO (G-PPO, Ablation 2)*: We implement GUIDEd PPO [56], incorporating TSUMs and agent uncertainty into the state representation, to examine the effect of the underlying RL algorithm on GUIDE’s performance.

2) *Baselines*: We compare GUIDE against several baselines:

*SAC-Based Methods*. We include SAC variants that handle uncertainty differently:

- (i) *RL with Uncertainty Penalization (SAC-P)*: We modify the reward function in SAC to penalize high uncertainty:  $R_{\text{SAC-P}} = R_{\text{base}} - \zeta u(s)$ , where  $R_{\text{base}}$  includes task rewards and localization costs,  $\zeta$  is a weighting factor, and  $u(s)$  is the agent’s current uncertainty. This tests traditional reward shaping versus GUIDE’s approach.
- (ii) *Bootstrapped Uncertainty-Aware RL (B-SAC)*: We implement Bootstrapped SAC [29], training multiple value networks to estimate epistemic uncertainty, which guides exploration and decision-making.
- (iii) *Heuristic Policy (HEU)*: A hand-crafted policy where the agent plans using SAC but switches to exact position estimation near obstacles or task-critical regions.

*Other Methods*. Additional baselines include:

- (iv) *Risk-Aware RL (CVaR)*: We train agents using a CVaR-based RL algorithm [24], optimizing a risk-sensitive



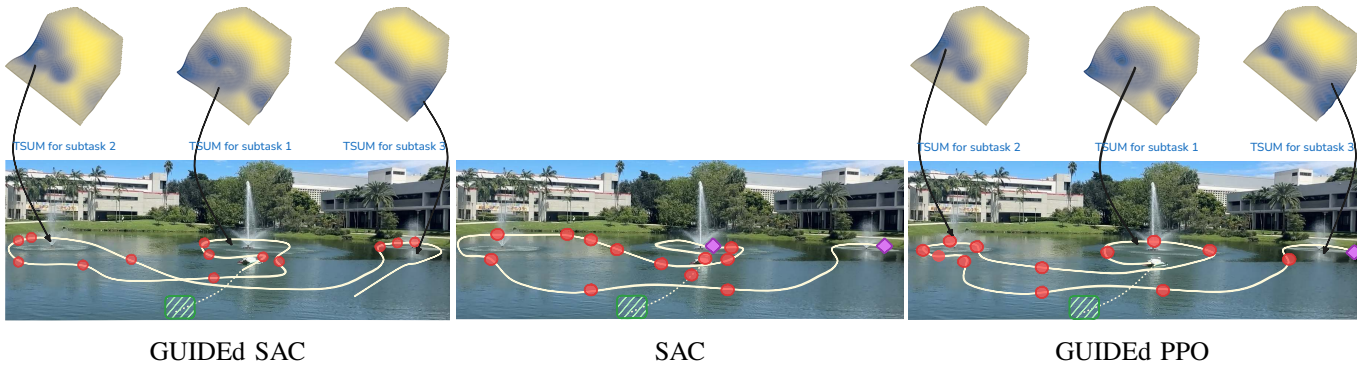


Fig. 4: Comparison of navigation trajectories on the task: Start at the dock, navigate around the central fountain, then around the left fountain, and finally around the right fountain. The white line represents the ASV’s trajectory, with red points marking locations where it reduced uncertainty to meet task-specific requirements. Pink diamonds indicate collision points, the green rectangle marks the starting dock, and the TSUMs for GUIDEd agents are shown above their respective figures.

Tasks	Metric	SAC	SAC-P	B-SAC	CVaR	RAA	HEU	G-PPO	G-SAC
<b>Goal reaching: waypoint</b> visit [coordinate]	TCR (%) (↑)	67.2%	82.1%	75.9%	68.8%	35.3%	71.3%	83.8%	95.7%
	Reward (avg) (↑)	186.2	260.4	249.5	184.8	26.9	176.1	319.0	429.2
<b>Goal reaching: context</b> navigate to dock	TCR (%) (↑)	68.9%	84.3%	74.2%	66.8%	32.7%	73.5%	81.7%	91.5%
	Reward (avg) (↑)	144.1	241.8	189.2	134.6	53.5	137.5	308.3	400.2
<b>Avoid tasks</b> avoid the central fountain	TCR (%) (↑)	71.3%	83.2%	79.6%	78.4%	51.3%	62.4%	89.6%	87.4%
	Reward (avg) (↑)	177.8	199.2	277.6	220.4	107.8	174.4	437.6	480.2
<b>Perimeter tasks</b> go around the left fountain	TCR (%) (↑)	44.3%	51.6%	56.3%	41.6%	39.8%	49.6%	74.9%	85.6%
	Reward (avg) (↑)	84.4	132.8	170.4	32.8	111.2	146.8	449.2	599.6
<b>Explore tasks</b> explore top-right quadrant	TCR (%) (↑)	88.6%	92.4%	87.6%	84.9%	71.3%	88.7%	93.8%	97.3%
	Reward (avg) (↑)	486	474	526	449	402	537	548	595
<b>Restricted areas</b> visit dock while avoiding top-right quadrant	TCR (%) (↑)	70.8%	82.1%	78.4%	71.2%	51.1%	63.9%	90.0%	88.6%
	Reward (avg) (↑)	266.4	306.8	307.2	269.6	201.4	261.2	570.0	634.6
<b>Multi-goal tasks</b> Combination of tasks (see Fig. 3)	TCR (%) (↑)	31.3%	42.9%	37.7%	30.9%	19.5%	42.1%	72.8%	81.7%
	Reward (avg) (↑)	124.4	135.2	122.4	129.2	100.4	155.2	423.6	510.4

TABLE I: Performance comparison between GUIDE and baseline methods on Task Completion Rate (TCR) and average cumulative reward, across different task categories. Results are averaged over 50 experiments per task category. Example tasks are provided below each task category to illustrate the types of navigation challenges evaluated.

objective to minimize potential high-cost outcomes, focusing on worst-case scenarios without task-specific uncertainty levels.

- (v) *Uncertainty-Aware Motion Planning (RAA)*: We employ Risk-Aware A\* [20] to plan paths that minimize collision probabilities under uncertainty, aiming for overall uncertainty minimization without considering task-specific requirements.

### C. Results

The performance of GUIDE compared to various baseline methods is summarized in Table I<sup>3</sup>. Our results demonstrate that GUIDE consistently outperforms all baselines across all task categories. Notably, both GUIDEd Actor-Critic (G-SAC) and GUIDEd PPO (G-PPO) outperform the baselines; however, G-SAC generally achieves higher task completion rates and rewards.

#### 1) Analysis of Ablation Studies:

- a) *Impact of TSUMs (Ablation 1)*: To assess the significance of incorporating Task-Specific Uncertainty Maps

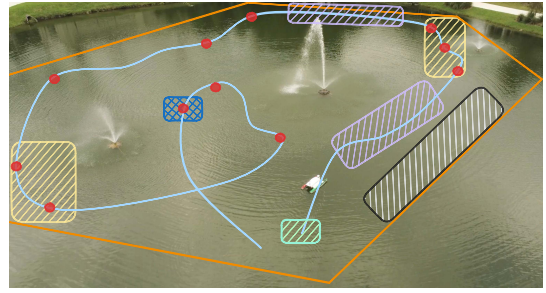
<sup>3</sup>Extensive additional experiment results can be found in the appendix and the video supplementary.

(TSUMs), we compare the standard Soft Actor-Critic (SAC) without TSUMs to GUIDEd Actor-Critic (G-SAC). As shown in Table I, conditioning on TSUMs significantly enhances performance across all tasks. Without TSUMs, SAC cannot manage positional uncertainty in a task-specific manner, leading to suboptimal navigation decisions and lower rewards. To further illustrate the effect of TSUM integration, we present in Fig. 4 the trajectories of agents with and without TSUMs on a representative task. We observe that SAC often overuses high-precision localization in areas where it is unnecessary, incurring additional costs without significant benefits. Conversely, in critical regions requiring precise navigation, SAC fails to reduce uncertainty appropriately, leading to collisions with the fountains. In contrast, the G-SAC agent effectively uses TSUMs to adapt its uncertainty management, switching to high-precision localization in areas where the TSUM indicates low acceptable uncertainty. This enables the agent to navigate safely around obstacles and complete tasks more efficiently.

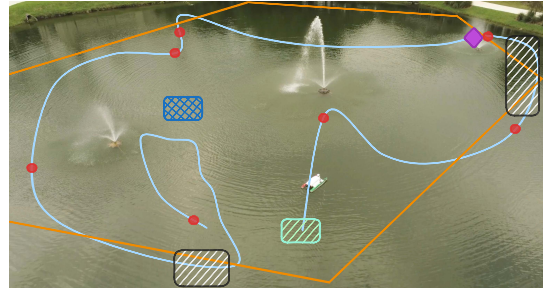
b) *Effect of RL Algorithm Choice (Ablation 2):* We also investigate the impact of the underlying reinforcement learning algorithm by comparing GUIDEd PPO (G-PPO) to G-SAC, both of which integrate TSUMs but differ in their RL methodologies. This difference in the performance of G-SAC and G-PPO can be attributed to several factors inherent to the algorithms. G-SAC, based on the SAC framework, is an off-policy method that leverages entropy regularization to encourage exploration while maintaining stability. Its off-policy nature allows for more efficient sample utilization, which is particularly beneficial in continuous action spaces and when data collection is costly or limited. In contrast, PPO is an on-policy algorithm that relies on proximal updates to prevent large policy shifts, using a clipped objective function. While PPO is stable, it can be less sample-efficient [34], as it requires new data for each policy update and may not explore as effectively in complex environments.

Our empirical results suggest that the off-policy efficiency and exploration capabilities of G-SAC make it better suited for navigation tasks. Furthermore, the entropy term in G-SAC encourages the agent to consider a wider range of actions, enabling it to discover more optimal strategies for managing uncertainty in a task-specific context.

2) *Comparison with Baselines:* GUIDE consistently outperforms all baselines across task types in both task completion rate and average reward (see Table I). Standard RL methods like SAC and SAC-P lack task-specific uncertainty management. SAC-P penalizes high uncertainty uniformly, resulting in overly conservative behavior where precision is unnecessary and insufficient caution in critical regions, ultimately leading to lower performance. B-SAC estimates epistemic uncertainty but fails to adapt to task-specific requirements, leading to inefficient exploration. Risk-Aware RL methods like CVaR are uniformly risk-averse, missing opportunities for calculated risk-taking that could improve task success. RAA aims to minimize overall uncertainty without considering task context, often generating inefficient paths. The Heuristic Policy (HEU) switches to exact localization near obstacles,



GUIDEd SAC



SAC-P

Fig. 5: Comparison of navigation trajectories between GUIDEd SAC and SAC-P agents on the task: Start and end at the dock. Go around the perimeter of the area and visit coordinates [redacted for paper anonymity]. The light blue line represents the trajectory taken by the agent. Red dots indicate locations where the agent actively reduced its state estimation uncertainty. The green rectangle denotes the dock, blue rectangle marks the specific coordinates the agent is instructed to visit.

but lacks GUIDE’s adaptability, failing to adjust to sudden changes in uncertainty requirements.

3) *Behavior of GUIDEd Agents:* We observed distinct behaviors in GUIDEd agents across various tasks. Analyzing the specific task shown in Fig. 5, GUIDEd agents strategically adjust their reliance on precise position estimation versus noisier estimates. In areas where the TSUMs indicate high precision is necessary — such as navigating near obstacles or close to the perimeters (Fig. 5, highlighted in yellow) — the agents opt for exact positioning despite the higher operational cost. Conversely, in less critical regions (Fig. 5, highlighted in purple), they rely on less precise, noisy estimates. This adaptability allows GUIDEd agents to manage uncertainty more efficiently than baselines, resulting in faster completion times and smoother trajectories. Although not perfect — occasionally missing sections of the perimeter (indicated by black shaded regions in Fig. 5) — GUIDEd agents significantly outperform baselines like SAC-P with engineered rewards. Baseline methods, lacking adaptive uncertainty management, frequently fail to complete tasks safely. They often collide with obstacles (pink diamond highlighted in Fig. 5) or take inefficient paths (Fig. 5 black highlighted region).

## V. LIMITATIONS

While GUIDE demonstrates promising results, several limitations should be noted. First, the current implementation assumes static uncertainty requirements and may not adapt well to environments where acceptable uncertainty levels change rapidly. Second, the framework relies heavily on the quality of image and may face challenges in environments with bad-quality visual data. Third, while our approach effectively handles a wide range of navigation tasks, it may require additional consideration for scenarios where task specifications are inherently ambiguous or contain multiple valid interpretations of uncertainty requirements.

## VI. CONCLUSION

In this paper, we introduced GUIDE, a framework that integrates task-specific uncertainty requirements into robotic navigation policies for limited-localization environments. Central to our approach is the concept of Task-Specific Uncertainty Maps (TSUMs), which represent acceptable levels of state estimation uncertainty across different regions of the environment based on the given task. By conditioning navigation policies on TSUMs, we enable robots to reason about the context-dependent importance of certainty and adapt their behavior accordingly.

We demonstrated how GUIDE can be incorporated into reinforcement learning frameworks by augmenting the state representation to include both the acceptable uncertainty levels from TSUMs and the robot's current state estimation uncertainty. Specifically, we adapted the Soft Actor-Critic (SAC) algorithm to operate in this augmented state space, resulting in the GUIDEd SAC algorithm. Our extensive experiments demonstrate GUIDE's effectiveness through successful in-the-wild deployments across various previously unseen environments, showing significant improvements in task completion rates and overall performance compared to baseline methods that do not explicitly consider task-specific uncertainty.

The results indicate that incorporating task-specific uncertainty requirements allows robots to effectively balance task objectives with appropriate uncertainty management. GUIDE enhances navigation strategies by enabling robots to focus their uncertainty reduction efforts where it is most critical for task success, leading to improved efficiency. Future work includes extending the framework to handle dynamic environments where uncertainty requirements may change over time.

## REFERENCES

- [1] Mohammad Alali and Mahdi Imani. Bayesian reinforcement learning for navigation planning in unknown environments. *Frontiers in Artificial Intelligence*, 2024.
- [2] Chenjia Bai, Lingxiao Wang, Zhuoran Yang, Zhihong Deng, Animesh Garg, Peng Liu, and Zhaoran Wang. Pessimistic bootstrapping for uncertainty-driven offline reinforcement learning. *arXiv preprint arXiv:2202.11566*, 2022.
- [3] Matthew Budd, Paul Duckworth, Nick Hawes, and Bruno Lacerda. Bayesian reinforcement learning for single-episode missions in partially unknown environments. In *Conference on Robot Learning*, 2023.
- [4] Matthew Chang, Theophile Gervet, Mukul Khanna, Sriram Yenamandra, Dhruv Shah, So Yeon Min, Kavitha Shah, Chris Paxton, Saurabh Gupta, Dhruv Batra, et al. GOAT: Go to any thing. *arXiv preprint arXiv:2311.06430*, 2023.
- [5] Tao Chen, Saurabh Gupta, and Abhinav Gupta. Learning exploration policies for navigation. *arXiv preprint arXiv:1903.01959*, 2019.
- [6] Yinlam Chow, Mohammad Ghavamzadeh, Lucas Janson, and Marco Pavone. Risk-constrained reinforcement learning with percentile risk criteria. *Journal of Machine Learning Research*, 2018.
- [7] Gerald Cook and Feitian Zhang. *Mobile robots: Navigation, control and sensing, surface robots and AUVs*. John Wiley & Sons, 2020.
- [8] Aidan Curtis, George Matheos, Nishad Gothoskar, Vikash Mansinghka, Joshua Tenenbaum, Tomás Lozano-Pérez, and Leslie Pack Kaelbling. Partially observable task and motion planning with uncertainty and risk awareness. *arXiv preprint arXiv:2403.10454*, 2024.
- [9] Carlos Florensa, David Held, Xinyang Geng, and Pieter Abbeel. Automatic goal generation for reinforcement learning agents. In *International conference on machine learning*, 2018.
- [10] Sébastien Forestier, Rémy Portelas, Yoan Mollard, and Pierre-Yves Oudeyer. Intrinsically motivated goal exploration processes with automatic curriculum learning. *Journal of Machine Learning Research*, 2022.
- [11] Dieter Fox, Sebastian Thrun, Wolfram Burgard, and Frank Dellaert. Particle filters for mobile robot localization. In *Sequential Monte Carlo methods in practice*. Springer, 2001.
- [12] Alejandro Gonzalez-Garcia and Herman Castañeda. Guidance and control based on adaptive sliding mode strategy for a usv subject to uncertainties. *IEEE Journal of Oceanic Engineering*, 2021.
- [13] Faiza Gul, Wan Rahiman, and Syed Sahal Nazli Alhady. A comprehensive study for robot navigation techniques. *Cogent Engineering*, 2019.
- [14] Siyu Guo, Xiuguo Zhang, Yiquan Du, Yisong Zheng, and Zhiying Cao. Path planning of coastal ships based on optimized DQN reward function. *Journal of Marine Science and Engineering*, 2021.
- [15] Fredrik Gustafsson, Fredrik Gunnarsson, Niclas Bergman, Urban Forssell, Jonas Jansson, Rickard Karlsson, and P-J Nordlund. Particle filters for positioning, navigation, and tracking. *IEEE Transactions on signal processing*, 2002.
- [16] Fredrik Gustafsson, Fredrik Gunnarsson, Niclas Bergman, Urban Forssell, Jonas Jansson, Rickard Karlsson, and P-J Nordlund. Particle filters for positioning, navigation, and tracking. *IEEE Transactions on signal processing*, 2002.

- [17] Tuomas Haarnoja, Aurick Zhou, Pieter Abbeel, and Sergey Levine. Soft actor-critic: Off-policy maximum entropy deep reinforcement learning with a stochastic actor. In *International conference on machine learning*, 2018.
- [18] Astghik Hakobyan, Gyeong Chan Kim, and Insoon Yang. Risk-aware motion planning and control using cvar-constrained optimization. *IEEE Robotics and Automation letters*, 2019.
- [19] Marc Hanheide, Moritz Göbelbecker, Graham S Horn, Andrzej Pronobis, Kristoffer Sjöo, Alper Aydemir, Patric Jensfelt, Charles Gretton, Richard Dearden, Miroslav Janicek, et al. Robot task planning and explanation in open and uncertain worlds. *Artificial Intelligence*, 2017.
- [20] Chuanhui Hu and Yan Jin. Long-range risk-aware path planning for autonomous ships in complex and dynamic environments. *Journal of Computing and Information Science in Engineering*, 2023.
- [21] Wenlong Huang, Fei Xia, Dhruv Shah, Danny Driess, Andy Zeng, Yao Lu, Pete Florence, Igor Mordatch, Sergey Levine, Karol Hausman, et al. Grounded decoding: Guiding text generation with grounded models for robot control. *arXiv preprint arXiv:2303.00855*, 2023.
- [22] Jeffrey Hudack. *Risk-aware planning for sensor data collection*. PhD thesis, Syracuse University, 2016.
- [23] Nivre Joakim. An efficient algorithm for projective dependency parsing. In *8th International Workshop on Parsing Technologies*, 2003, 2003.
- [24] Gregory Kahn, Adam Villaflor, Vitchyr Pong, Pieter Abbeel, and Sergey Levine. Uncertainty-aware reinforcement learning for collision avoidance. *arXiv preprint arXiv:1702.01182*, 2017.
- [25] Jonathan Ko and Dieter Fox. GP-BayesFilters: Bayesian filtering using gaussian process prediction and observation models. *Autonomous Robots*, 2009.
- [26] Henrik Kretzschmar, Markus Spies, Christoph Sprunk, and Wolfram Burgard. Socially compliant mobile robot navigation via inverse reinforcement learning. *The International Journal of Robotics Research*, 2016.
- [27] Jonáš Kulhánek, Erik Derner, and Robert Babuška. Visual navigation in real-world indoor environments using end-to-end deep reinforcement learning. *IEEE Robotics and Automation Letters*, 2021.
- [28] Aviral Kumar, Justin Fu, Matthew Soh, George Tucker, and Sergey Levine. Stabilizing off-policy Q-Learning via bootstrapping error reduction. *Advances in neural information processing systems*, 2019.
- [29] Aviral Kumar, Justin Fu, Matthew Soh, George Tucker, and Sergey Levine. Stabilizing off-policy Q-Learning via bootstrapping error reduction. *Advances in neural information processing systems*, 2019.
- [30] Charline Le Lan, Stephen Tu, Mark Rowland, Anna Harutyunyan, Rishabh Agarwal, Marc G Bellemare, and Will Dabney. Bootstrapped representations in reinforcement learning. *arXiv preprint arXiv:2306.10171*, 2023.
- [31] Min-Fan Ricky Lee and Sharfiden Hassen Yusuf. Mobile robot navigation using deep reinforcement learning. *Processes*, 2022.
- [32] Guofa Li, Yifan Yang, Shen Li, Xingda Qu, Nengchao Lyu, and Shengbo Eben Li. Decision making of autonomous vehicles in lane change scenarios: Deep reinforcement learning approaches with risk awareness. *Transportation research part C: emerging technologies*, 2022.
- [33] Yueming Li, Mingquan Ma, Jian Cao, Guobin Luo, Depeng Wang, and Weiqiang Chen. A method for multi-uv cooperative area search in unknown environment based on reinforcement learning. *Journal of Marine Science and Engineering*, 2024.
- [34] Shijie Liu. An evaluation of DDPG, TD3, SAC, and PPO: Deep reinforcement learning algorithms for controlling continuous system. In *2023 International Conference on Data Science, Advanced Algorithm and Intelligent Computing (DAI 2023)*. Atlantis Press, 2024.
- [35] Björn Lütjens, Michael Everett, and Jonathan P How. Safe reinforcement learning with model uncertainty estimates. In *2019 International Conference on Robotics and Automation*, 2019.
- [36] Corey Lynch, Mohi Khansari, Ted Xiao, Vikash Kumar, Jonathan Tompson, Sergey Levine, and Pierre Sermanet. Learning latent plans from play. In *Conference on robot learning*, 2020.
- [37] Christoforos Mavrogiannis, Francesca Baldini, Allan Wang, Dapeng Zhao, Pete Trautman, Aaron Steinfeld, and Jean Oh. Core challenges of social robot navigation: A survey. *ACM Transactions on Human-Robot Interaction*, 2023.
- [38] Steven Morad, Ryan Kortvelesy, Matteo Bettini, Stephan Liwicki, and Amanda Prorok. POPGym: Benchmarking partially observable reinforcement learning. *arXiv preprint arXiv:2303.01859*, 2023.
- [39] Kevin P Murphy. Bayesian map learning in dynamic environments. *Advances in neural information processing systems*, 1999.
- [40] Ashvin V Nair, Vitchyr Pong, Murtaza Dalal, Shikhar Bahl, Steven Lin, and Sergey Levine. Visual reinforcement learning with imagined goals. *Advances in neural information processing systems*, 2018.
- [41] Ashvin V Nair, Vitchyr Pong, Murtaza Dalal, Shikhar Bahl, Steven Lin, and Sergey Levine. Visual reinforcement learning with imagined goals. *Advances in neural information processing systems*, 2018.
- [42] Masahiro Ono, Thoams J Fuchs, Amanda Steffy, Mark Maimone, and Jeng Yen. Risk-aware planetary rover operation: Autonomous terrain classification and path planning. In *2015 IEEE aerospace conference*, 2015.
- [43] Ian Osband, Charles Blundell, Alexander Pritzel, and Benjamin Van Roy. Deep exploration via bootstrapped DQN. *Advances in neural information processing systems*, 2016.
- [44] Alvaro Ovalle and Simon M Lucas. Bootstrapped model learning and error correction for planning with uncer-

- tainty in model-based rl. In *2020 IEEE Conference on Games*, 2020.
- [45] Abhishek Padalkar, Acorn Pooley, Ajinkya Jain, Alex Bewley, Alex Herzog, Alex Irpan, Alexander Khazatsky, Anant Rai, Anikait Singh, Anthony Brohan, et al. Open X-Embodiment: Robotic learning datasets and RT-X models. *arXiv preprint arXiv:2310.08864*, 2023.
- [46] Utsav Patel, Nithish K Sanjeev Kumar, Adarsh Jagan Sathyamoorthy, and Dinesh Manocha. DWA-RL: Dynamically feasible deep reinforcement learning policy for robot navigation among mobile obstacles. In *2021 IEEE International Conference on Robotics and Automation*, 2021.
- [47] BK Patle, Anish Pandey, DRK Parhi, AJDT Jagadeesh, et al. A review: On path planning strategies for navigation of mobile robot. *Defence Technology*, 2019.
- [48] Niklas Paulig and Ostap Okhrin. Robust path following on rivers using bootstrapped reinforcement learning. *Ocean Engineering*, 2024.
- [49] Gokul Puthumanaim, Manav Vora, and Melkior Ornik. ComTraQ-MPC: Meta-trained dqn-mpc integration for trajectory tracking with limited active localization updates. *arXiv preprint arXiv:2403.01564*, 2024.
- [50] Alec Radford, Jong Wook Kim, Chris Hallacy, Aditya Ramesh, Gabriel Goh, Sandhini Agarwal, Girish Sastry, Amanda Askell, Pamela Mishkin, Jack Clark, et al. Learning transferable visual models from natural language supervision. In *International Conference on Machine Learning*, pages 8748–8763. PMLR, 2021.
- [51] Kate Rakelly, Aurick Zhou, Chelsea Finn, Sergey Levine, and Deirdre Quillen. Efficient off-policy meta-reinforcement learning via probabilistic context variables. In *International conference on machine learning*, 2019.
- [52] Krishan Rana, Ben Talbot, Vibhavari Dasagi, Michael Milford, and Niko Sünderhauf. Residual reactive navigation: Combining classical and learned navigation strategies for deployment in unknown environments. In *2020 IEEE International Conference on Robotics and Automation*, 2020.
- [53] Cesar A Rojas, Paulo Padrão, Jose Fuentes, Gregory M Reis, Arif R Albayrak, Batuhan Osmanoglu, and Leonardo Bobadilla. Combining multi-satellite remote and in-situ sensing for unmanned underwater vehicle state estimation. *Ocean Engineering*, 310:118708, 2024.
- [54] Gerard Salton. Modern information retrieval. (*No Title*), 1983.
- [55] Erik F Sang and Fien De Meulder. Introduction to the conll-2003 shared task: Language-independent named entity recognition. *arXiv preprint cs/0306050*, 2003.
- [56] John Schulman, Filip Wolski, Prafulla Dhariwal, Alec Radford, and Oleg Klimov. Proximal policy optimization algorithms. *arXiv preprint arXiv:1707.06347*, 2017.
- [57] Wilko Schwarting, Javier Alonso-Mora, and Daniela Rus. Planning and decision-making for autonomous vehicles. *Annual Review of Control, Robotics, and Autonomous Systems*, 2018.
- [58] Dhruv Shah, Michael Robert Equi, Błażej Osiniński, Fei Xia, Brian Ichter, and Sergey Levine. Navigation with large language models: Semantic guesswork as a heuristic for planning. In *Conference on Robot Learning*, 2023.
- [59] Dhruv Shah, Błażej Osiniński, Sergey Levine, et al. Lmnav: Robotic navigation with large pre-trained models of language, vision, and action. In *Conference on robot learning*, 2023.
- [60] Dhruv Shah, Ajay Sridhar, Arjun Bhorkar, Noriaki Hirose, and Sergey Levine. GNM: A general navigation model to drive any robot. In *2023 IEEE International Conference on Robotics and Automation*, 2023.
- [61] Dhruv Shah, Ajay Sridhar, Nitish Dashora, Kyle Stachowicz, Kevin Black, Noriaki Hirose, and Sergey Levine. ViNT: A foundation model for visual navigation. *arXiv preprint arXiv:2306.14846*, 2023.
- [62] Siddharth Singi, Zhanpeng He, Alvin Pan, Sandip Patel, Gunnar A Sigurdsson, Robinson Piramuthu, Shuran Song, and Matei Ciocarlie. Decision making for human-in-the-loop robotic agents via uncertainty-aware reinforcement learning. In *2024 IEEE International Conference on Robotics and Automation*, 2024.
- [63] Matthijs TJ Spaan, Tiago S Veiga, and Pedro U Lima. Decision-theoretic planning under uncertainty with information rewards for active cooperative perception. *Autonomous Agents and Multi-Agent Systems*, 29:1157–1185, 2015.
- [64] Krishnan Srinivasan, Benjamin Eysenbach, Sehoon Ha, Jie Tan, and Chelsea Finn. Learning to be safe: Deep RL with a safety critic. *arXiv preprint arXiv:2010.14603*, 2020.
- [65] Annalisa T Taylor, Thomas A Berrueta, and Todd D Murphey. Active learning in robotics: A review of control principles. *Mechatronics*, 2021.
- [66] Sebastian Thrun. Particle filters in robotics. In *UAI*, 2002.
- [67] Ning Wang, Yabiao Wang, Yuming Zhao, Yong Wang, and Zhigang Li. Sim-to-real: Mapless navigation for usvs using deep reinforcement learning. *Journal of Marine Science and Engineering*, 2022.
- [68] Xin Wang, Qiuyuan Huang, Asli Celikyilmaz, Jianfeng Gao, Dinghan Shen, Yuan-Fang Wang, William Yang Wang, and Lei Zhang. Reinforced cross-modal matching and self-supervised imitation learning for vision-language navigation. In *Proceedings of the IEEE/CVF conference on computer vision and pattern recognition*, 2019.
- [69] Zixiang Wang, Hao Yan, Zhuoyue Wang, Zhengjia Xu, Zhizhong Wu, and Yining Wang. Research on autonomous robots navigation based on reinforcement learning. In *3rd International Conference on Robotics, Artificial Intelligence and Intelligent Control*, pages 78–81. IEEE, 2024.
- [70] Zifan Xu, Bo Liu, Xuesu Xiao, Anirudh Nair, and Peter Stone. Benchmarking reinforcement learning techniques for autonomous navigation. In *2023 IEEE International*

*Conference on Robotics and Automation*, 2023.

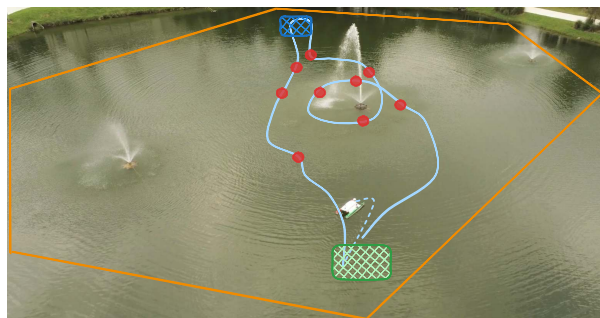
- [71] Denis Yarats, Amy Zhang, Ilya Kostrikov, Brandon Amos, Joelle Pineau, and Rob Fergus. Improving sample efficiency in model-free reinforcement learning from images. In *Proceedings of the AAAI conference on artificial intelligence*, 2021.
- [72] Kexiong Curtis Zeng, Shinan Liu, Yuanchao Shu, Dong Wang, Haoyu Li, Yanzhi Dou, Gang Wang, and Yaling Yang. All your GPS are belong to us: Towards stealthy manipulation of road navigation systems. In *27th USENIX security symposium (USENIX security 18)*, 2018.
- [73] Yu Zhang, Sarath Sreedharan, Anagha Kulkarni, Tathagata Chakraborti, Hankz Hankui Zhuo, and Subbarao Kambhampati. Plan explicability for robot task planning. In *Proceedings of the RSS Workshop on Planning for Human-Robot Interaction: Shared Autonomy and Collaborative Robotics*, 2016.
- [74] Zhiqian Zhou, Zhiwen Zeng, Lin Lang, Weijia Yao, Huimin Lu, Zhiqiang Zheng, and Zongtan Zhou. Navigating robots in dynamic environment with deep reinforcement learning. *IEEE Transactions on Intelligent Transportation Systems*, 2022.
- [75] CY Zhu. Intelligent robot path planning and navigation based on reinforcement learning and adaptive control. *Journal of Logistics, Informatics and Service Science*, 2023.
- [76] Kai Zhu and Tao Zhang. Deep reinforcement learning based mobile robot navigation: A review. *Tsinghua Science and Technology*, 2021.
- [77] Yuanyang Zhu, Zhi Wang, Chunlin Chen, and Daoyi Dong. Rule-based reinforcement learning for efficient robot navigation with space reduction. *IEEE/ASME Transactions on Mechatronics*, 2021.
- [78] Yuke Zhu, Roozbeh Mottaghi, Eric Kolve, Joseph J Lim, Abhinav Gupta, Li Fei-Fei, and Ali Farhadi. Target-driven visual navigation in indoor scenes using deep reinforcement learning. In *2017 IEEE international conference on robotics and automation*, 2017.
- [79] P Zieliński and Urszula Markowska-Kaczmar. 3d robotic navigation using a vision-based deep reinforcement learning model. *Applied Soft Computing*, 2021.

## APPENDIX

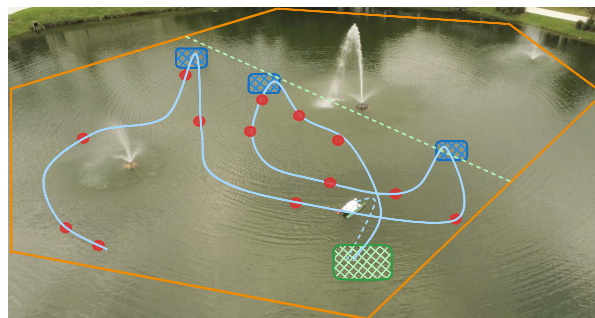
This supplementary material provides:

- *Additional Experimental Results*: Extended evaluations of GUIDE on various tasks.
- *Implementation Details*: Descriptions of the dataset, model architectures and hyperparameters for GUIDE and all baselines.
- *PFA Video Demonstrations*: Selected experimental runs are included in the accompanying video.

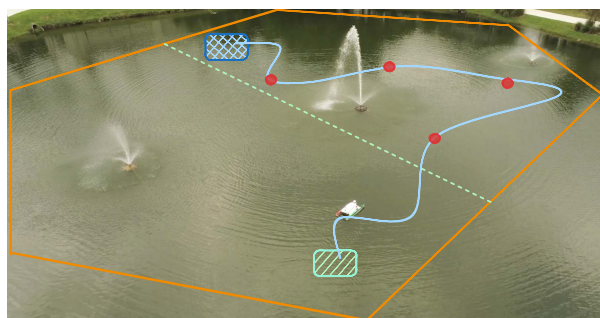
### VII. ADDITIONAL EXPERIMENTAL RESULTS



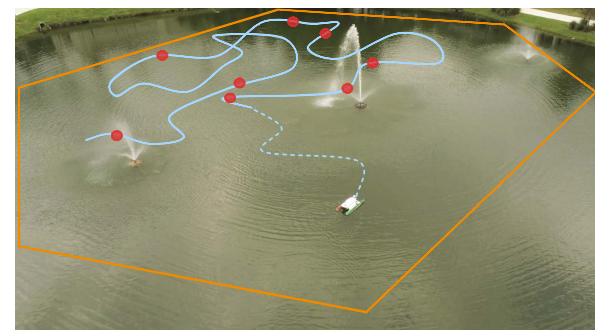
(a) "Go to point  $[80,90]$  and then go around the central fountain and return to the dock."



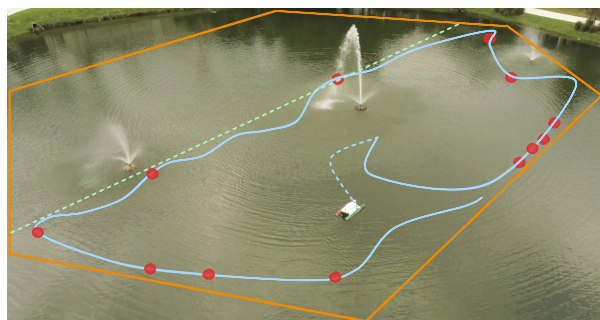
(b) "Go to  $[80,60]$  and then go to  $[80,20]$  and then go to  $[80,70]$  and finally return to the dock. This task has to be completed by avoiding the right half of the area."



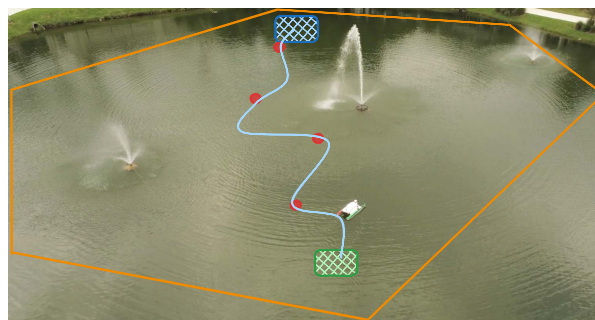
(c) "Go to  $[40,60]$  while avoiding the left half of the environment."



(d) "Explore the top half of the environment."



(e) "Navigate the perimeter of the bottom half of the lake."



(f) "Go to  $[40,60]$ ."

Fig. 6: Illustrations of various navigation tasks performed by GUIDED SAC in the environment. In all images, the light blue line represents the trajectory, red dots indicate areas where uncertainty was reduced, the green rectangle represents the dock, and brown rectangles represent waypoints that need to be reached. The specific tasks are described below each figure.

Note: the coordinates mentioned in the illustrations and the examples are dummy values to maintain anonymity.

## A. Implementation Details

1) *Task Categories and Examples*: The tasks in the dataset are grouped into six categories, each designed to test specific aspects of navigation and uncertainty management. Below, we describe each category in detail and provide representative examples.

a) *Goal Reaching: Waypoint*: This category involves tasks where the ASV is instructed to navigate to specific coordinates. The focus is on reaching designated points in the environment.

Examples:

- Navigate to waypoint (12.0, -7.5).
- Proceed to the coordinates (8.5, 15.0).
- Go to the location at (5.0, -10.0).

b) *Goal Reaching: Contextual Landmarks*: This category includes tasks where the ASV is instructed to navigate to locations identified by contextual landmarks rather than explicit coordinates. This tests the ability to interpret semantic information and associate it with spatial positions.

Examples:

- Go to the dock.
- Proceed to the central fountain.
- Navigate to the area in front of the left fountain.

c) *Avoidance Tasks*: These tasks instruct the ASV to avoid certain points or areas, emphasizing obstacle detection and path planning to circumvent specified locations.

Examples:

- Avoid the coordinates (10.0, -5.0).
- Steer clear of the submerged rock at (3.5, 4.0).

d) *Perimeter Navigation Tasks*: In this category, the ASV is tasked with navigating around the perimeter of a specified area. This requires maintaining a certain distance from boundaries.

Examples:

- Navigate around the perimeter of the bottom-right quadrant.
- Circumnavigate the central fountain.
- Traverse the boundary of the entire lake.

e) *Exploration Tasks*: These tasks involve exploring a specified area for a fixed duration of 5 minutes, testing the ASV's ability to stay within an area and cover parts.

Examples:

- Explore the top-half of the lake.
- Conduct an exploration of the top-right quadrant.

f) *Restricted Area Navigation*: Tasks in this category require the ASV to navigate while avoiding specified regions.

Examples:

- Go to waypoint (6.0, -3.0) while avoiding the right half of the lake.
- Navigate to the right fountain, avoiding the exclusion zone.
- Proceed to the dock without passing through the left half of the lake.

2) *Natural Language Processing and Embedding Generation*: To process the natural language task descriptions, we utilized a fine-tuned RoBERTa language model, which captures contextual nuances and effectively handles synonyms and varied phrasings. This enables the model to interpret different expressions of similar tasks, ensuring robustness to linguistic variations. For example, phrases like 'proceed to', 'navigate to', and 'go to' are recognized as equivalent in intent.

The semantic embeddings generated by RoBERTa are paired with spatial embeddings derived from the associated coordinates or landmarks, allowing the model to learn meaningful associations between language and location. This approach ensures that even when new tasks are presented with different wording or synonyms, the model can generalize and generate appropriate Task-Specific Uncertainty Maps.

3) *Dataset and Data Processing*: The dataset used for training our TSUM generation model consists of overhead imagery collected from various marine environments and simulation scenes, carefully curated to capture a wide range of operational scenarios. The data collection process spanned multiple weather conditions to ensure robustness and generalizability of the trained model.

For the labeling process, we employed experts with experience in autonomous navigation. These experts followed an annotation protocol to maintain consistency across the dataset. The protocol involved examining each 224×224 pixel patch of overhead imagery and assigning binary labels indicating relevance to predefined subtasks and constraints. The labeling criteria were established through iterative refinement to ensure practical applicability.



To address class imbalance issues in our dataset, we implemented a comprehensive sampling strategy. Many critical navigation scenarios, such as complex docking maneuvers or navigation around certain obstacles, were naturally underrepresented in the raw data collection. We addressed this through strategic oversampling of these crucial but rare scenarios. Specifically, patches containing these underrepresented classes were duplicated in the training set, while maintaining cross-validation splits to prevent overfitting. For negative examples, we employed a systematic sampling approach, randomly selecting patches that domain experts had deemed irrelevant to specific subtasks or constraints, while ensuring a balanced representation across different environmental conditions.

The environmental variations in our dataset were curated to capture the diverse conditions encountered in real-world marine operations. Our collection includes patches from both real-world lake environments and high-fidelity simulated scenarios. The real-world data encompasses variations in weather conditions (clear, overcast, and light rain), lighting conditions (morning, midday, and evening), and seasonal changes affecting water conditions. Shoreline features vary from natural boundaries to man-made structures, and obstacle density ranges from sparse open waters to crowded marina environments. The simulated data complements these real-world scenarios by providing additional coverage of rare but critical scenarios that are difficult to capture in real-world data collection.

For data storage and organization, we implemented a metadata management system. Each image patch is stored in a georeferenced index using a custom CSV format, which maintains associations between image patches, their geographical coordinates, and corresponding labels. This schema ensures efficient retrieval during training and enables seamless integration with existing robotic navigation systems. The metadata includes essential information such as timestamp, environmental conditions, and annotation confidence scores from domain experts.

Our data augmentation pipeline was designed to enhance model robustness while preserving critical visual cues for marine navigation. The primary augmentations include random rotations (in 90-degree increments) and horizontal flips, which reflect the rotational invariance of navigation tasks while maintaining the natural appearance of water features. Notably, we deliberately avoided color jittering and intensity transformations, as these could distort important water-related visual cues that are crucial for accurate navigation. The augmentation parameters were tuned through extensive experimentation to find the optimal balance between increasing data diversity and maintaining task-relevant features. All image patches undergo consistent preprocessing to ensure uniformity in the training data. This includes standardization to zero mean and unit variance, computed across the training set, and resizing to maintain consistent spatial resolution across different source imagery. The preprocessing pipeline also includes automated quality checks to identify and filter out patches with excessive noise, sensor artifacts, or poor visibility conditions that could negatively impact model training.

4) *Technical Infrastructure and Hardware Setup:* Our technical infrastructure was designed to efficiently handle the computational demands of processing large-scale overhead imagery and training complex neural networks. The foundation of our data processing pipeline centers on the conversion of geographical coordinates to discrete 224×224 pixel patches, which serve as the basic unit of analysis for our TSUM generation system. The coordinate-to-patch mapping system employs a gridding algorithm that subdivides large overhead maps into a regular grid of fixed-size patches. Each patch is assigned center coordinates that correspond to real-world geographical positions. The mapping process utilizes a custom spatial indexing structure that enables efficient lookup of relevant patches given any arbitrary location in the operational space. To handle edge cases where locations fall between patch boundaries, we implemented a nearest-center assignment strategy that ensures every point in the operational space maps to exactly one patch while maintaining spatial continuity.

To maximize processing efficiency, we developed a parallelized data generation pipeline. The system utilizes a custom-built multithreaded tiling script that leverages all available CPU cores to concurrently process large imagery datasets. This parallelization is implemented using Python’s multiprocessing library, with careful attention to memory management to prevent resource exhaustion when handling particularly large maps. The tiling process is coordinated by a master thread that manages work distribution and ensures balanced load across all available processors. Each worker thread independently processes assigned regions of the input imagery, generating patches and associated metadata in parallel.

The runtime environment is built on Ubuntu 20.04 LTS with CUDA 11.8 and cuDNN 8.7, optimized for deep learning workloads. We utilize Docker containers to ensure consistency across different compute nodes and to simplify deployment. The container images are based on NVIDIA’s NGC PyTorch container, customized with additional dependencies required for our specific workload. This containerized approach ensures reproducibility and enables easy scaling across different hardware configurations. Data movement between storage and compute nodes is optimized using a custom data loading pipeline built on top of PyTorch’s DataLoader class. We implemented prefetching mechanisms that load and preprocess data for upcoming batches while the current batch is being processed on the GPUs. This approach effectively hides I/O latency and ensures near-continuous GPU utilization. The data loading pipeline includes automatic checkpointing to enable recovery from system failures without losing progress.

The typical processing workflow for a complete dataset involves approximately 2-3 hours of initial data tiling and preprocessing, followed by 10 epochs of model training. The training process is distributed using PyTorch’s DistributedDataParallel, with gradient synchronization optimized for our specific network architecture and batch sizes. Our implementation achieves

approximately 71% GPU utilization during training, with the remaining overhead primarily attributed to necessary data loading operations.

Resource monitoring and system health checks are performed using a combination of Prometheus for metrics collection and Grafana for visualization. This monitoring infrastructure allows us to track system performance, identify bottlenecks, and optimize resource utilization in real-time. Additionally, we maintain comprehensive logs of all processing steps, enabling detailed analysis of system performance and facilitating debugging when necessary.

A crucial component of our technical infrastructure is our high-fidelity simulation environment, built using Unity3D (2022.3.16f1) in conjunction with ROS2 Humble. This simulator serves as a vital tool for both data generation and policy validation. The Unity environment provides physically accurate water dynamics for fluid simulation, capable of modeling complex wave patterns, water resistance, and hydrodynamic forces. We implemented custom shaders to accurately render water surface properties, ensuring visual fidelity crucial for training vision-based navigation systems.

The simulator is tightly integrated with ROS2 through a custom bridge that enables bidirectional communication between Unity and ROS2 nodes. This integration allows for seamless transfer of sensor data, control commands, and state information. We implemented the full suite of sensors found on our physical ASV, including simulated GPS (with configurable noise patterns), IMU (with drift characteristics matching real hardware), and cameras (with accurate lens distortion and environmental effects). The simulator also includes detailed models of environmental factors such as wind effects, current patterns, and varying lighting conditions.

For training data generation, the simulator can be run in a distributed headless manner across instances, each generating different scenarios and environmental conditions. We used an off-shelf scenario generation system that creates diverse training situations, including varying obstacle configurations, weather conditions, and traffic patterns. The simulator supports both synchronous and asynchronous operation modes, allowing for rapid data collection when generating training datasets and real-time operation when validating policies.

## B. Hyperparameters

Hyperparameter Name	Brief Explanation	Value
<b>TSUM Aggregation</b>		
$w_\Phi$	Weight for subtask relevance function $\Phi^\tau(l)$	0.5
$w_C$	Weight for constraint relevance $C^\tau(l)$	0.3
$w_\mathcal{E}$	Weight for environmental factors $\mathcal{E}(l)$	0.2
<b>CLIP Fine-Tuning</b>		
CLIP embedding dimension $d$	Output dimension of ViT-B/32 encoders (text/image)	512
Number of frozen layers	Initial layers in CLIP left frozen to retain general cross-modal knowledge	6
Fine-tuning epochs	Epochs used to adapt the unfrozen CLIP layers	10
Learning rate for CLIP	LR for training the unfrozen CLIP layers	$1 \times 10^{-5}$
Alignment weighting $\lambda_{\text{align}}$	Weight on additional alignment loss $\mathcal{L}_{\text{align}}$	1.0
Contrastive temperature $\zeta$	Temperature hyperparameter for CLIP contrastive loss	0.07
<b>Reinforcement Learning (SAC)</b>		
Discount factor $\gamma$	Discount factor in the RL objective	0.99
Initial temperature $\alpha$	Initial entropy temperature in SAC	0.2
Target entropy $\bar{\mathcal{H}}$	Target policy entropy term in SAC	-2
Soft target update $\tau$	Polyak averaging coefficient for target Q-networks	0.005
Replay buffer size $ \mathcal{D} $	Maximum capacity of the experience replay buffer	$1 \times 10^6$
Batch size	Number of samples per RL training batch	256
Learning rate for policy network	LR for optimizing the policy $\pi_\theta$	$3 \times 10^{-4}$
Learning rate for Q-value networks	LR for optimizing the Q-value functions $Q_{\phi_i}$	$3 \times 10^{-4}$
Learning rate for temperature $\alpha$	LR for adjusting the SAC temperature	$3 \times 10^{-4}$
Policy network architecture	MLP for $\pi_\theta$ with hidden layers and activation	2 layers, 256 units each, ReLU
Q-value networks architecture	MLP for $Q_{\phi_i}$ , identical structure	2 layers, 256 units each, ReLU
Maximum steps per episode	Upper bound on steps in each training episode	1000

TABLE II: Hyperparameters for the CLIP-based TSUM generation and SAC policy learning.

Hyperparameter Name	Brief Explanation	Value
<b>1. Standard RL without TSUMs (SAC, Ablation 1)</b>		
State representation	The agent uses only the original state $s$	
<b>2. GUIDEd PPO (G-PPO, Ablation 2)</b>		
Policy optimization algorithm	Proximal Policy Optimization (PPO) is used instead of SAC	
Clip ratio $\epsilon$	Clipping parameter for PPO policy updates	0.2
Number of epochs per update	Number of epochs per policy update iteration	10
Learning rate for policy and value networks	Learning rate for updating network parameters	$3 \times 10^{-4}$
Generalized Advantage Estimation lambda $\lambda_{GAE}$	Smoothing parameter for advantage estimation	0.95
Batch size	Number of samples per training batch	64
State representation	Augmented state $\tilde{s} = [s, U^\tau(s), u(s)]$	
<b>3. RL with Uncertainty Penalization (SAC-P)</b>		
Penalty weight $\zeta$	Weighting factor for uncertainty penalization in the reward function $R_{SAC-P} = R_{base} - \zeta u(s)$	0.4
State representation	Original state $s$	
<b>4. Bootstrapped Uncertainty-Aware RL (B-SAC)</b>		
Number of bootstrap heads	Number of Q-value networks used to estimate epistemic uncertainty	10
Bootstrap sampling probability	Probability of selecting each head during training	0.8
Uncertainty estimation method	Standard deviation across bootstrap heads	
State representation	Original state $s$	
<b>5. Heuristic Policy (HEU)</b>		
Switching threshold distance	Distance to obstacles or task-critical regions at which the agent switches to exact position estimation	3.5 meters
Planning algorithm	Base planning using SAC	
Exact position estimation mode	The mode $\eta$ used for precise localization when close to obstacles	$\eta = 1$
State representation	Original state $s$	
<b>6. Risk-Aware RL (CVaR)</b>		
Risk level $\alpha_{CVaR}$	Conditional Value at Risk (CVaR) level, determining the quantile of worst-case outcomes considered	0.05
CVaR optimization method	Optimization of the expected value over the worst $\alpha_{CVaR}$ fraction of outcomes	CVaR objective
State representation	Original state $s$	
<b>7. Uncertainty-Aware Motion Planning (RAA)</b>		
Acceptable collision probability $p_{collision}$	Threshold probability of collision acceptable during planning	0.01
Risk assessment horizon	Number of steps ahead considered for risk assessment	50

TABLE III: Hyperparameters for the baseline and abalation methods. Unless specified, methods use the same hyperparameters as in GUIDEd SAC (see Table II). Only differences from GUIDEd SAC are listed for each method.